

## Prompt $\alpha$ Decay of a Well-Deformed Band in $^{58}\text{Ni}$

D. Rudolph,<sup>1</sup> C. Baktash,<sup>2</sup> M. Devlin,<sup>3,\*</sup> D. R. LaFosse,<sup>3,†</sup> L. L. Riedinger,<sup>4</sup> D. G. Sarantites,<sup>3</sup> and C.-H. Yu<sup>2</sup>

<sup>1</sup>*Department of Physics, Lund University, S-22100 Lund, Sweden*

<sup>2</sup>*Physics Division, Oak Ridge National Laboratory, Oak Ridge, Tennessee 37831*

<sup>3</sup>*Chemistry Department, Washington University, St. Louis, Missouri 63130*

<sup>4</sup>*Department of Physics, University of Tennessee, Knoxville, Tennessee 37996*

(Received 8 February 2000; revised manuscript received 16 October 2000)

Two excited well-deformed bands have been observed in the semi-magic nucleus  $^{58}\text{Ni}$ . One of the bands was observed to partially decay by emission of a prompt discrete  $\alpha$  particle that feeds the 2949 keV  $6^+$  spherical yrast state in the daughter nucleus  $^{54}\text{Fe}$ . This constitutes the first observation of prompt  $\alpha$  emission from states lying in the deformed secondary minimum of the nuclear potential.  $\gamma$ -ray linking transitions via several parallel paths establish the spin, parity, and excitation energy of this deformed band in  $^{58}\text{Ni}$ .

DOI: 10.1103/PhysRevLett.86.1450

PACS numbers: 23.60.+e, 21.60.Cs, 23.20.Lv, 27.40.+z

Alpha radioactivity was first explained in 1908 by Rutherford in terms of nuclear decay by emission of a  $^4\text{He}$  nucleus [1]. Later,  $\alpha$  emission was found to be the most common mode of decay for the ground states of nuclei heavier than lead. Similarly,  $\alpha$  emission from discrete excited states has been observed in several nuclei situated two neutrons beyond the  $N = 82$  and  $N = 126$  magic numbers. The half-lives of these  $\alpha$ -emitting states range from approximately a nanosecond (e.g., the  $6^+$  state in  $^{212}\text{Po}$  [2]) to millions of years (e.g., the  $9^-$  state in  $^{210}\text{Bi}$  [3]). The factors that affect the  $\alpha$ -decay probabilities are the  $\alpha$  formation factor, tunneling penetration through the Coulomb barrier, and overlap of the wave functions of the parent and daughter nuclei [4,5].

States in the second minimum of the nuclear potential corresponding to very elongated or superdeformed shapes were first observed in the actinide region [6]. They were found to decay by either  $\gamma$  rays into the first well of the potential, or by spontaneous fission. Though small  $\alpha$ -decay branches from these shape isomers are theoretically possible [7], none have been firmly established until now. (Recently, a long-lived activity in  $^{210}\text{Fr}$  has been claimed to represent such a decay mode [8].) This possibility, however, could be enhanced in light and medium-mass nuclei where the Coulomb barrier is lower. In fact, we recently reported on the observation of prompt monoenergetic proton decays from well-deformed states in the second wells of  $^{56}\text{Ni}$  [9] and  $^{58}\text{Cu}$  [10] into spherical daughter states. In this Letter, we report on the first observation of a prompt discrete  $\alpha$ -decay branch from a well-deformed state in the second minimum of the nucleus  $^{58}\text{Ni}$  into the spherical 2949 keV  $6^+$  yrast state in the daughter nucleus  $^{54}\text{Fe}$ .

In the past, mainly light-ion induced reactions were used to study excited states in  $^{58}\text{Ni}$  [11]. Recently, a high-spin study established excited states up to about 8 MeV and spin  $I \sim 10 \hbar$  [12]. We investigated excited states in  $^{58}\text{Ni}$  using the heavy-ion fusion reaction  $^{28}\text{Si}(^{36}\text{Ar}, 1\alpha 2p)$  at 143 MeV beam energy. About 1/3 of the total cross

section in this reaction led to  $^{58}\text{Ni}$  residues. The experiment used the GAMMASPHERE Ge-detector array [13] in conjunction with the  $4\pi$  charged-particle detector system MICROBALL [14]. More detailed information about the experimental setup, data reduction, and the analysis methods may be found in Ref. [15].

Coincidence, intensity balance, and summed energy relations were used to establish an extensive high-spin level scheme of  $^{58}\text{Ni}$  which comprises more than 100 states connected by some 250  $\gamma$ -ray transitions [16]. A small portion of this level scheme that is relevant to the prompt  $\alpha$  decay of  $^{58}\text{Ni}$  to the low-spin yrast sequence of  $^{54}\text{Fe}$  [15] is shown in Fig. 1. Both rotational bands (labeled 1 and 2) extend over five transitions, and are connected by interband transitions at 1171 and 1503 keV. The intensities of the bands, relative to the 1454 keV ground-state transition, are  $\sim 2\%$  and  $\sim 1\%$ , respectively. The weak 1364 and 1385 keV transitions depopulating the level at 16795 keV are candidates for the continuation of band 1 towards lower spins. They account for 25(10)% of the intensity of the 1663 keV line. The decays of the corresponding ( $13^-$ ) states, however, could not be resolved. We also observed two high-energy single-step linking transitions at 3750 and 3964 keV into the irregularly spaced states in the spherical first minimum. In total, we find 67(12)% of the yield of the 1663 keV line in seven depopulating discrete  $\gamma$ -ray transitions, while the sum of the yields of the 1171 and 1663 keV transitions account for about 75% of that of the 1989 keV line. The band-head of band 2 is depopulated by the 4288 keV link which carries only 10% of the yield of the 1685 keV transition. Figure 2(a) shows the sum of  $1\alpha 2p$ -gated  $\gamma$ -ray spectra in coincidence with the 1663, 1989, and 2350 keV transitions (band 1). The high-energy peaks at 3750, 3848, 3964, and 4288 keV are marked in the inset. We have also labeled several well-known  $^{58}\text{Ni}$  transitions (537, 842, 1005, 1161, 1454, and 2668 keV) [11,12], as well as important peaks relevant to the  $\alpha$  decay of band 1 (Fig. 1).

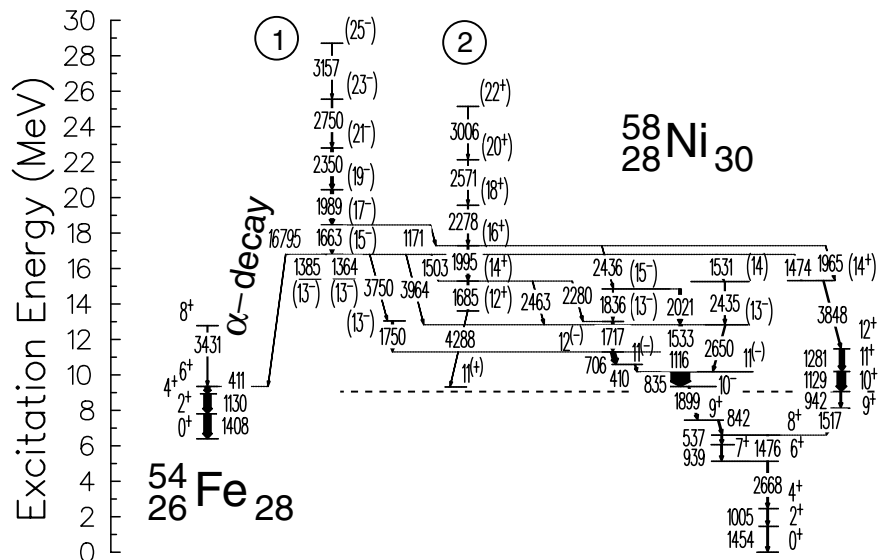


FIG. 1. A partial level scheme for  $^{58}\text{Ni}$  and low-spin yrast sequence of  $^{54}\text{Fe}$ . The  $\gamma$ -ray labels are given in keV. The widths of the arrows are proportional to their relative intensities above the dashed line at 9 MeV excitation energy. The excitation energy is measured relative to the ground state of  $^{58}\text{Ni}$ .

Assignments of spins and parities of the excited levels were based on the analysis of  $1\alpha 2p$ -gated directional  $\gamma\gamma$  correlations of oriented states ( $R_{\text{DCO}}$ ) and  $\gamma$ -coincident angular distribution data, as outlined in Ref. [15]. Transitions in the bands and the most intense linking transition at 3964 keV showed DCO ratios  $R_{\text{DCO}} \sim 1.0$ , consistent

with stretched quadrupole character. The two interband transitions, however, showed values of  $R_{\text{DCO}} \sim 0.5$ , similar to the values for the intense 706 and 1116 keV transitions in the first minimum, which have stretched dipole character. It should be stressed that the high level of interleaving  $\gamma$  rays puts additional constraints on the proposed spin assignments. Using the residual Doppler shift method [17], an average quadrupole moment of  $\overline{Q}_i = 2.4(3)$  eb for band 1 was deduced. Assuming that the 1364 and 1385 keV lines with their summed branching of 25(10)% form the continuation of band 1 to lower spins and that the quadrupole moment remains constant, a mean lifetime of  $\tau = 10$ –40 fs may be estimated for the 16 795 keV state.

Most interestingly, the 16 795 keV state in band 1 was found to decay via a 3.9(3)% discrete  $\alpha$  branch into the 2949 keV  $6^+$  yrast state in the daughter nucleus  $^{54}\text{Fe}$ . In fact, the subsequent  $\gamma$  rays at 411, 1130, and 1408 keV are visible in Fig. 2(a). However, since the  $^{54}\text{Fe} + 2\alpha 2p$  reaction channel leaks into the  $1\alpha 2p$ -gate spectrum when one  $\alpha$  particle escapes detection, this coincidence could be due to the contaminating lines in  $^{54}\text{Fe}$  [15]. Moreover, weak 410, 1129, and 1404 keV transitions also appear in the extensive level scheme of  $^{58}\text{Ni}$ . They are in coincidence with band 1 (cf. Fig. 1 and Ref. [16]).

Nevertheless, there is strong evidence for the existence of a discrete  $\alpha$  branch which is summarized in Figs. 2(b) and 3. First of all, we restricted our analysis to  $\alpha$  particles detected in the first four rings of the MICROBALL. This leads to a reduction of  $\alpha$  detection efficiency from  $\epsilon_\alpha = 65(1)\%$  to 51(1)%, but implies unambiguous particle identifications and energies [18]. Second, the  $Q$  value of the presumed  $\alpha$  decay amounts to 7.45 MeV [19], of which 0.55 MeV is lost to the kinetic energy of the recoiling  $^{54}\text{Fe}$

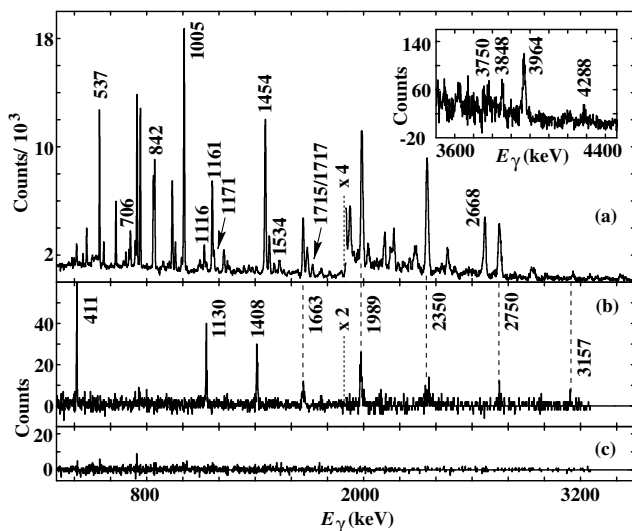


FIG. 2. (a) Sum of the  $\gamma$ -ray spectra of  $^{58}\text{Ni}$  in coincidence with the lowest three transitions in band 1 and gated by one  $\alpha$  particle and two protons. The inset shows the high-energy portion of the spectrum. (b) Same as (a) but also in coincidence with any of the lowest three transitions in the  $^{54}\text{Fe}$  yrast cascade, and an additional  $\alpha$  particle which had to be detected in rings 1–4 of MICROBALL. At least one of the two  $\alpha$  particles was required to have  $E_{\alpha, \text{c.m.}} < 8$  MeV. (c) Same as (b) but in coincidence with the 1005 and 1454 keV transitions in  $^{58}\text{Ni}$  instead of those from the  $^{54}\text{Fe}$  cascade.

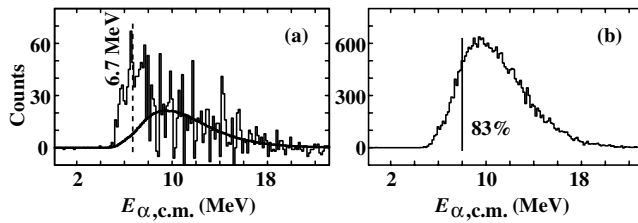


FIG. 3. Sums of  $\alpha$  energy spectra in coincidence with any of the lowest three  $\gamma$ -ray transitions in  $^{54}\text{Fe}$  and one of the three lowest transitions of band 1 (a), or an additional transition in  $^{54}\text{Fe}$  (b) [15]. For comparison, a normalized spectrum of panel (b) is shown as solid line in panel (a). The vertical dashed line in (a) indicates the peak position.

residue. Taking into account the kinematic broadening of the  $\alpha$  peak [10,18], an upper limit of  $E_{\alpha,c.m.} = 8$  MeV may be inferred beyond which  $\alpha$  particles are *not* associated with the new decay mode.

Figure 2(b) shows a  $\gamma$ -ray spectrum gated by two protons and two  $\alpha$  particles, at least one of which was required to have an energy of  $E_{\alpha,c.m.} < 8$  MeV. This figure is the sum of nine spectra in double coincidence with (i) one of the 411, 1130, and 1408 keV transitions in  $^{54}\text{Fe}$  and (ii) one of the 1663, 1989, and 2350 keV transitions in band 1 of  $^{58}\text{Ni}$ . Clearly, the only additional peaks in Fig. 2(b) are the other two transitions in band 1. In particular, all other transitions from  $^{58}\text{Ni}$  are absent [cf. Fig. 2(a)]. The relative intensities of the 411, 1130, and 1408 keV lines amount to 100(7), 99(9), and 95(8)%, respectively, in the sum of the three spectra coincident with condition (ii) only. Consequently, there is no apparent experimental evidence for the population of any other than the 2949 keV  $6^+$  yrast state in  $^{54}\text{Fe}$  via the  $\alpha$  decay. For Fig. 2(c) condition (i) was replaced with the 1454 and 1005 keV transitions in  $^{58}\text{Ni}$ . This spectrum provides a reference background since such events should never occur except for pileup.

Figure 3(a) is the center-of-mass  $\alpha$ -energy spectrum,  $E_{\alpha,c.m.}$ , for  $2\alpha 2p$ -gated events, subject to the same double- $\gamma$ -coincidence requirements as in Fig. 2(b). This spectrum reveals a peak at 6.7(2) MeV, which is consistent with the above mentioned  $Q$  value. It should be contrasted against the spectrum in Fig. 3(b) which required coincidence with (iii) one of the 780, 2097, and 2979 keV  $\gamma$  rays known in  $^{54}\text{Fe}$  [15], instead of (ii) one of the transitions in band 1 of  $^{58}\text{Ni}$ . The latter spectrum has a distribution expected for evaporated particles. To highlight the excess under the 6.7(2) MeV peak, we have superimposed a normalized spectrum of panel (b) as a solid line on the spectrum in panel (a). The full width at half maximum (FWHM  $\sim 2.0$  MeV) of the peak is due to kinematic broadening rather than the intrinsic resolution of the MICROBALL elements [18].

In Fig. 4 we have plotted yield ratios of the *third*  $\gamma$  rays in  $2\alpha 2p$ -gated spectra with and without an  $E_{\alpha,c.m.} < 8$  MeV cutoff on the energy of at least one of the two  $\alpha$  particles. The two  $\gamma$  gates again correspond to (i) one of

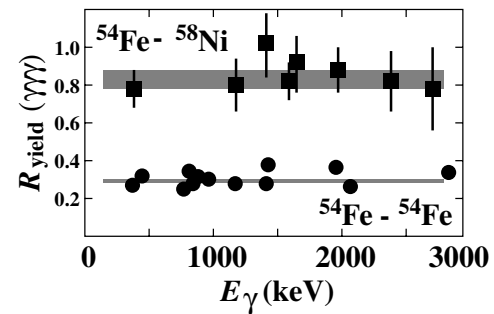


FIG. 4. Ratios of yields of  $\gamma$  rays. See text for details.

the 411, 1130, or 1408 keV transitions in  $^{54}\text{Fe}$  and either (ii) one of the transitions in band 1 of  $^{58}\text{Ni}$  (filled squares labeled as  $^{54}\text{Fe}-^{58}\text{Ni}$ ), or (iii) one of the above mentioned transitions in  $^{54}\text{Fe}$  (filled circles labeled as  $^{54}\text{Fe}-^{54}\text{Fe}$ ). Though the  $^{54}\text{Fe}-^{58}\text{Ni}$  data points should reach unity, the slight mismatch [ $R_{\text{yield}} = 0.83(4)$ ] can be attributed to the loss of the high-energy fraction of the peak in Fig. 3(a). The statistics for  $^{54}\text{Fe}-^{54}\text{Fe}$  coincidences are significantly reduced, because we have lost events where *both*  $\alpha$  particles exceeded the imposed  $E_{\alpha,c.m.}$  cutoff value. Since 83% of the  $\alpha$  particles have energies in excess of 8 MeV [cf. Fig. 3(b)], one expects  $R_{\text{yield}} = 1.0 - 0.83^2 = 0.31$  for  $^{54}\text{Fe}-^{54}\text{Fe}$  coincidences, in perfect agreement with Fig. 4. These observations finally confirm that the source of the  $^{54}\text{Fe}$   $\gamma$  rays in Fig. 2(b) is the  $\alpha$  decay of band 1 [18].

The branching ratio  $b_\alpha$  of the  $\alpha$  emission may be determined by measuring the ratio  $R$  of the yields of the band in  $1\alpha 2p$ - and  $2\alpha 2p$ -gated spectra. Here one has to consider the leak-through of  $^{58}\text{Ni}$  into the first gate due to pileup in the charged-particle array. This ratio was estimated to be  $R(\text{normal}) = 0.13(1)\%$  for numerous transitions from the normally deformed states in  $^{58}\text{Ni}$ , versus  $R(\text{band1}) = 1.8(1)\%$  for band 1. The yield  $Y_2$  of band 1 in  $2\alpha 2p$ -gated spectra amounts to

$$Y_2 = \epsilon_\alpha^2 b_\alpha R_{\text{yield}} \quad (1)$$

as we imply the above mentioned 8-MeV energy cutoff to work under conditions as clean as possible. The yield  $Y_1$  of band 1 in  $1\alpha 2p$ -gated spectra comprises two terms, namely  $\alpha$  decays of the band for which we missed the detection of one of the two  $\alpha$  particles, and conventional  $\gamma$  decays of band 1. Using  $b_\gamma = 1 - b_\alpha$  one obtains

$$Y_1 = 2\epsilon_\alpha(1 - \epsilon_\alpha)b_\alpha + \epsilon_\alpha(1 - b_\alpha). \quad (2)$$

With  $R_{21} = R(\text{band1}) - R(\text{normal}) = Y_2/Y_1$  it is possible to determine  $b_\alpha$  by combining Eqs. (1) and (2):

$$b_\alpha = \frac{R_{21}}{\epsilon_\alpha R_{\text{yield}} - R_{21}(1 - 2\epsilon_\alpha)} = 3.9(3)\%. \quad (3)$$

This is in excellent agreement with the  $b_\alpha = 4(2)\%$  value which was alternatively estimated from Fig. 2(b)

by accounting for the  $\gamma$ -ray doublets and comparing the efficiency-corrected yields of the 1454 keV ground-state transition in  $^{58}\text{Ni}$  with the averaged yield of the three transitions in  $^{54}\text{Fe}$ . Using the above estimate of  $\tau = 10\text{--}40$  fs for the 16795 keV state, a value of 0.25–1.0 ps for the partial half-life of the  $\alpha$  branch may be inferred. Finally, the angular distribution of the  $\alpha$  peak is found similarly pronounced as that of evaporated  $\alpha$  particles. This suggests a spin change of  $\Delta l \sim 7\text{--}9 \hbar$  corresponding to the average angular momentum carried away by  $\alpha$  particles from the compound system.

Based on predictions from Skyrme Hartree-Fock calculations a configuration can be assigned to band 1 [20], for which two of the 30 neutrons and one of the 28 protons of  $^{58}\text{Ni}$  occupy the  $\mathcal{N} = 4$   $g_{9/2}$  [440]1/2 intruder Routhians, while one of the [321]1/2 or [312]5/2 levels in the  $fp$  shell is empty. This assignment to band 1 is based on the predicted near yrast nature in the respective excitation energy and spin regime, and the spin alignments relative to the band in  $^{58}\text{Cu}$  [20].

The observation of the  $\alpha$  decay of band 1 suggests that the parent nucleus has a considerable overlap with a state composed by an  $\alpha$  particle and a spherical daughter nucleus. A detailed calculation of the  $\alpha$ -decay width in terms of microscopic formation factor, Coulomb penetration, and the spectroscopic factor, which shall in principle include the drastic shape change, is beyond the scope of the present experimental study. Nevertheless, a qualitative understanding of an  $\alpha$  decay appears to be possible based on a simple shell-model picture: The  $6^+$  state in the spherical daughter nucleus  $^{54}\text{Fe}$  consists of two-proton holes in the  $f_{7/2}$  orbital, while the 28 neutrons reveal the magic particle number. To achieve the largest possible overlap with respect to occupied orbits between the remaining 54 nucleons after the  $\alpha$  decay and the  $6^+$  state in  $^{54}\text{Fe}$ , it is clear that both  $1g_{9/2}$  neutrons and the  $1g_{9/2}$  proton have to be part of the  $\alpha$ . This is in line with the fact that the  $1g_{9/2}$  particles are shape driving, and move close to the surface of deformed  $A \sim 60$  nuclei. If the band configuration involved already a proton hole in the [312]5/2 orbit ( $m = 5/2$  of the  $1f_{7/2}$  shell), the second proton for the  $\alpha$  particle is likely to come from the [321]1/2 orbit ( $m = 1/2$  of the  $2p_{3/2}$  shell), since that needs to be emptied when changing from the deformed to the spherical shell model. In turn, if the band configuration had a hole in the [321]1/2 orbit, the second proton should come from the [312]5/2 orbit.

In summary, we have established two rotational bands in  $^{58}\text{Ni}$  which decay via several  $\gamma$  rays to spherical states in this nucleus. A weak 3.9(3)% discrete  $\alpha$  decay branch connects the 16795 keV ( $15^-$ ) state of band 1 with the spherical 2949 keV  $6^+$  yrast state in  $^{54}\text{Fe}$ . This consti-

tutes the first observation of prompt  $\alpha$  decay of a state associated with the deformed secondary minimum in the potential. Predicted band configurations and simple shell-model arguments suggest a consistent picture of this exotic decay mode.

We thank J. Dobaczewski for the kind permission to use the HF results and W. Nazarewicz for discussions. We gratefully acknowledge the excellent support during the experiment from LBNL GAMMASPHERE and operations staff. This research was supported by the Swedish Natural Science Research Council and the U.S. Department of Energy [Grants No. DE-FG02-96ER40963 (UT), and No. DE-FG05-88ER40406 (WU)]. ORNL is managed by Lockheed Martin Energy Research Corp. for the U.S. Department of Energy under Contract No. DE-AC05-96OR22464.

---

\*Present address: LANSCE-3, Los Alamos National Laboratory, Los Alamos, NM 87545.

†Present address: SUNY Stony Brook, Stony Brook, NY 11794.

- [1] E. Rutherford and H. Geiger, Proc. R. Soc. London **A81**, 162 (1908).
- [2] A. Artna-Cohen, Nucl. Data Sheets **66**, 171 (1992).
- [3] E. Browne, Nucl. Data Sheets **65**, 209 (1992).
- [4] E. U. Condon and R. W. Gurney, Nature (London) **122**, 439 (1928).
- [5] G. Gamow, Z. Phys. **51**, 204 (1928).
- [6] S. M. Polikanov *et al.*, Sov. Phys. JETP **15**, 1016 (1962).
- [7] S. Björnholm and J. E. Lynn, Rev. Mod. Phys. **52**, 725 (1980).
- [8] A. Marinov, S. Gelberg, and D. Kolb, Mod. Phys. Lett. A **11**, 861 (1996).
- [9] D. Rudolph *et al.*, Phys. Rev. Lett. **82**, 3763 (1999).
- [10] D. Rudolph *et al.*, Phys. Rev. Lett. **80**, 3018 (1998).
- [11] M. R. Bhat, Nucl. Data Sheets **80**, 789 (1997).
- [12] S. M. Vincent *et al.*, Phys. Rev. C **60**, 064308 (1999).
- [13] I.-Y. Lee, Nucl. Phys. **A520**, 641c (1990).
- [14] D. G. Sarantites *et al.*, Nucl. Instrum. Methods Phys. Res., Sect. A **381**, 418 (1996).
- [15] D. Rudolph *et al.*, Eur. Phys. J. **A4**, 115 (1999).
- [16] D. Rudolph *et al.* (to be published).
- [17] B. Cederwall *et al.*, Nucl. Instrum. Methods Phys. Res., Sect. A **354**, 591 (1995).
- [18] D. Rudolph, in *Nuclear Structure 98*, edited by C. Baktash, AIP Conf. Proc. No. 481 (AIP, New York, 1999), p. 192; in *The Nucleus: New Physics for the New Millennium*, edited by F. D. Smit, R. Lindsay, and S. V. Förtisch (Kluwer Academic/Plenum Publishers, New York, 2000), p. 397.
- [19] G. Audi and A. H. Wapstra, Nucl. Phys. **A565**, 1 (1993).
- [20] J. Dobaczewski *et al.* (private communication; to be published).